Hydration Structure of Antithrombin Conformers and Water Transfer during Reactive Loop Insertion

Jie Liang* and Maria P. McGee#

*National Center for Supercomputing Applications, University of Illinois at Urbana-Champaign, Urbana, Illinois 61807, and #Wake Forest University School of Medicine, Medicine Department, Rheumatology Section, Winston-Salem, North Carolina 27157 USA

ABSTRACT The serine protease inhibitor antithrombin undergoes extensive conformational changes during functional interaction with its target proteases. Changes include insertion of the reactive loop region into a β-sheet structure in the protein core. We explore the possibility that these changes are linked to water transfer. Volumes of water transferred during inhibition of coagulation factor Xa are compared to water-permeable volumes in the x-ray structure of two different antithrombin conformers. In one conformer, the reactive loop is largely exposed to solvent, and in the other, the loop is inserted. Hydration fingerprints of antithrombin (that is, water-permeable pockets) are analyzed to determine their location, volume, and size of access pores, using α shape-based methods from computational geometry. Water transfer during reactions is calculated from changes in rate with osmotic pressure. Hydration fingerprints prove markedly different in the two conformers. There is an excess of 61–76 water molecules in loop-exposed as compared to loop-inserted conformers. Quantitatively, rate increases with osmotic pressure are consistent with the transfer of 73 $\pm$ 7 water molecules. This study demonstrates that conformational changes of antithrombin, including loop insertion, are linked to water transfer from antithrombin to bulk solution. It also illustrates the combined use of osmotic stress and analytical geometry as a new and effective tool for structure/function studies.

INTRODUCTION

Antithrombin is a member of the serpin (serine protease inhibitor) family of protein inhibitors of proteases. It is the principal regulator of key coagulation proteases, including factor Xa and thrombin. In recent years, hypothetical models relating the structure and function of serpins have evolved from a vast body of structural, genetic, kinetic, immunologic, and biochemical evidence (for revisions see Olson and Bjork, 1994; Olds et al., 1994). Protease inhibition by serpins is initiated by a reversible interaction between residues at the active site of the protease and the reactive loop of the inhibitor. This initial interaction is followed by a formation of intermediates analogous to the catalytic complexes formed when protease hydrolyzes substrate. Cleavage of the reactive bond is arrested, and the protease is trapped in an equimolar, stable complex with serpin. Heparin and heparan sulfate glycosaminoglycans increase the equilibrium constant for the initial encounter between antithrombin and its target proteases, but do not affect the rate of the subsequent step(s) leading to stabilization of the complex.

Structural analysis of inhibitory and noninhibitory serpins suggests that the transition from the initial complex to the stable complex is associated with changes in the conformation of the inhibitor. For antithrombin, prevailing models postulate that the reactive loop is fully exposed to solvent during the initial encounter and becomes reinserted into a β-sheet structure in the protein core during the stabilizing transition (van Boekel et al., 1994). Whether extensive loop reinsertion is an absolute requirement for inhibition is still the subject of some controversy. Contradictory evidence from studies with mutant recombinant serpins supports both loop insertion and loop exclusion (Carrel and Stein, 1996).

The molecular structure of crystallized human antithrombin has been solved (Schreuder et al., 1994; Carrel et al., 1994). It consists of a complex of two antithrombin conformers. In one, the reactive loop is only partially inserted, with most of the reactive domain exposed to solvent. In the other, the reactive domain is completely inserted into the protein core. Coexistence of these two conformers in the crystals suggests that loop insertion is facilitated by dehydration during crystal formation and points to the possibility that water is transferred from the protein to bulk solution during reactions. Neither the distribution of water-permeable spaces in the x-ray structure of antithrombin nor the potential role of water transfer during reactions has been investigated before.

Water transfer during reactions can be studied under osmotic stress (OS), induced with inert cosolutes that are excluded from water-permeable spaces. Although proteins are well packed, hydrodynamic and NMR data indicate that in solution, proteins are associated with ~0.3–0.5 g of water/g of protein (Squire and Himmel, 1979). Cosolute exclusion from the water-permeable spaces in and between proteins (Bryant, 1996; Israelachvili and Wennerstrom, 1996) generates OS in the excluded spaces (Parsegian et al., 1995). Osmotic stress facilitates transfer of water from excluded spaces to bulk and opposes transfer from bulk to

Received for publication 12 September 1997 and in final form 22 April 1998.

Address reprint requests to Dr. Maria P. McGee, Wake Forest University, School of Medicine, Medicine Department, Rheumatology Section, Winston-Salem, NC 27157. Tel.: 336-716-6716; Fax: 336-716-9821; E-mail: mmcgee@bgsm.edu.

0006-3495/98/08/573/10 $2.00

excluded spaces. The rate of conformational transitions affecting the volume of excluded spaces is also influenced by OS (Rand, 1992). There is evidence indicating that the force mediating OS effects on proteins is transmitted across the solvent hydrogen-bond network (Kuznetsova et al., 1997).

In the present studies, we combine kinetic measurements under osmotic stress with structural analysis, using α shape methods from computational geometry (Eldesbrunner and Mucke, 1994) to examine structure/function relationships in antithrombin. α shape theory and methods are applied to the measurement and analysis of differences in the volume of water-permeable spaces shown by two distinct conformers resolved in antithrombin crystals. The volume differences between loop-exposed and loop-inserted conformer are found to correlate closely with the volume of water transferred during inhibition of coagulation factor Xa. This finding indicates that conformational transitions of antithrombin are water-linked and provides new independent evidence for extensive loop insertion during inhibition.

EXPERIMENTAL PROCEDURES

Analysis of water-permeable spaces: hydration fingerprints

Hydration fingerprints define the water-permeable spaces in a protein structure, their exact location and volumes, as well as the shape and area of the pores connecting them to bulk solvent. In this work, hydration fingerprints in the x-ray crystallography structures of antithrombin (PDB 1ant) are determined with the α shape method. The theoretical and computational aspects of this method have been described in detail before (Edelsbrunner and Mucke, 1994; Edelsbrunner et al., 1995, 1996). Briefly, the α shape is a geometrical object constructed from the set of points given by the structure's atomic coordinates. The procedure is based on triangulating the convex hull of the atoms' centers. Intuitively, the convex hull can be imagined as a tin foil surface wrapped tightly around the atoms' centers. Triangulation is the tiling, or covering up, of the convex hull with triangles so that there are no missing pieces or overlaps. To construct the α complex, the convex hull is subjected to Delaunay triangulation, a special type of tiling related to the Voronoi diagram. The Voronoi diagram is formed by a collection of cells, each consisting of the space closest to one atom (Richards, 1997; Gerstein et al., 1995). Two Voronoi cells meet at a face (a section of a plane), three meet at a line segment, and four meet at a vertex. The Voronoi diagram is mapped to the Delaunay triangulation by placing an edge connecting two neighboring atom centers for each Voronoi face; a triangle with vertices at three neighboring atom centers for each Voronoi line; and a tetrahedron with four neighboring atoms' centers at its corners for each Voronoi vertex. The Delaunay complex collects these tetrahedra, triangles, edges, etc. The α complex or α shape is a subset of the Delaunay complex, consisting of the vertices, line segments, and faces located within the atomic spheres. The difference between the Delaunay complex and the α complex reflects the empty spaces of the molecule (Liang et al., 1998a). These include voids, which appear inaccessible to solvent in the static picture represented by the structure, and pockets, which have openings or pores that allow access to and from the bulk solvent space. The empty spaces represented by tetrahedra are mapped further to the actual space-filling molecular surface (Connolly surface) or solvent-accessible surface. This correspondence is illustrated in Fig. 1, with the largest pocket in the loop-exposed conformer of antithrombin. Fig. 1 *A* shows the Delaunay tetrahedra that correspond to this pocket shaded in blue, except for the triangles corresponding to the access pore, which are shaded in gold. Fig. 1 *B* shows the same pocket in space-filling representation, with the atoms lining the concavity of the pocket in green. Among these, the atoms forming the rim of the access pore are shown in dark green. The volume of the pocket and the area of the pore can be computed analytically from the known dimensions of the tetrahedra by subtracting the volume occupied by atoms. Using the α complex, the three-dimensional shape of a protein can be defined at any resolution by varying a single parameter, α. This parameter is related to the van der Waals radius of each atom, r, by $r_\alpha = \sqrt{r^2 + \alpha^2}$. If the atoms' radii are inflated/deflated by giving values to α different from 0, different α complexes are generated, each representing the shape of the molecule at a different resolution. The different shape resolutions can be considered as the shape seen by probes of larger/smaller size. α shape has been applied to a variety of problems (Liang et al., 1998b; Kim et al., 1997; Liang and Subbranmaniam, 1997; Peters et al., 1996).

In this paper, the volume of water-permeable spaces excluded by cosolutes is calculated by subtracting the volumes probed by water (modeled as a sphere with 1.4-Å radius) from the volume probed by spheres with radii corresponding to the cosolute radius. The radius of cosolute PEG 300 (polyethylene glycol, with an average MW of 300) is estimated to be between 3 and 5.8 Å, from published equations (Atha and Ingham, 1981; Arakawa and Timasheff, 1985). Cosolute-excluded volumes are measured in the structures by using both values of the radius to model the probe. Software to compute α shapes, calculate volumes, and visualize water-permeable spaces is available from the National Center for Supercomputer Applications, University of Illinois at Urbana-Champaign.

The α shape method identifies and measures all pockets and cavities, providing information on volumes and pore areas that, to our knowledge, cannot be obtained with other software. Connolly's program can compute cavities analytically and has been applied to the calculation of pockets. In Connolly's approach, a probe of fixed radius is used to close up pores. However, a probe of fixed radius frequently misses a number of pockets; some have larger access pores and cannot be closed up, and some pockets become too small to accommodate the probe. Other programs using dots/cubes are numerical and subjective in nature. They cannot generate metric parameters and are very sensitive to the molecule's orientation. In addition, without the convex hull (as used in the α shape), determining where the pocket starts and the solvent spaces end is quite problematic. Algorithmically, α shape can handle atomic overlaps of more than four atoms. Multiple overlaps are common in complex structures, such as antithrombin. Connolly's and related algorithms ignore this high degree of overlap. Furthermore, the α shape deals with degeneracy without changing the input, and the method remains analytical and robust.

Measurement of factor Xa inhibition by antithrombin

Reaction rates are measured in mixtures of human antithrombin (10–440 nM), heparin (0.04–12 μg/ml, either commercial grade or fractionated, 1500 MW), and factor Xa (7–60 nM). Reagents are in Tris buffer, pH 7.2, with 0.07 N NaCl, 0.5% bovine serum albumin, and are equilibrated at 32°C. Sequential samples are withdraw from the mixtures at 5–300-s intervals (depending on heparin concentration) and diluted immediately in hexamethrine bromide. Residual protease activity is determined from the rate of substrate hydrolysis (methoxycarbonyl-D-cyclohexylglycil-arginine-*p*-nitroanilide-acetate) as described before (McGee and Li, 1991). Exponential decay equations are fitted to data points to calculate pseudo-first-order rate coefficients, k_{obs}. Second-order rate coefficients are determined from the initial slope of k_{obs} versus antithrombin concentration, at fixed concentrations of factor Xa and heparin. Control mixtures without antithrombin and/or heparin are included in each experiment.

Reaction rates are analyzed according to the following scheme, previously proposed and validated by other investigators (Olson et al., 1993):

$$\mathrm{AT-H + Xa} \overset{K}{\leftrightarrow} \mathrm{AT-H-Xa} \overset{k}{\rightarrow} \mathrm{AT-Xa + H}$$

where AT-H is the antithrombin-heparin complex, Xa is coagulation factor Xa, K is the dissociation constant for the interaction between antithrombin-

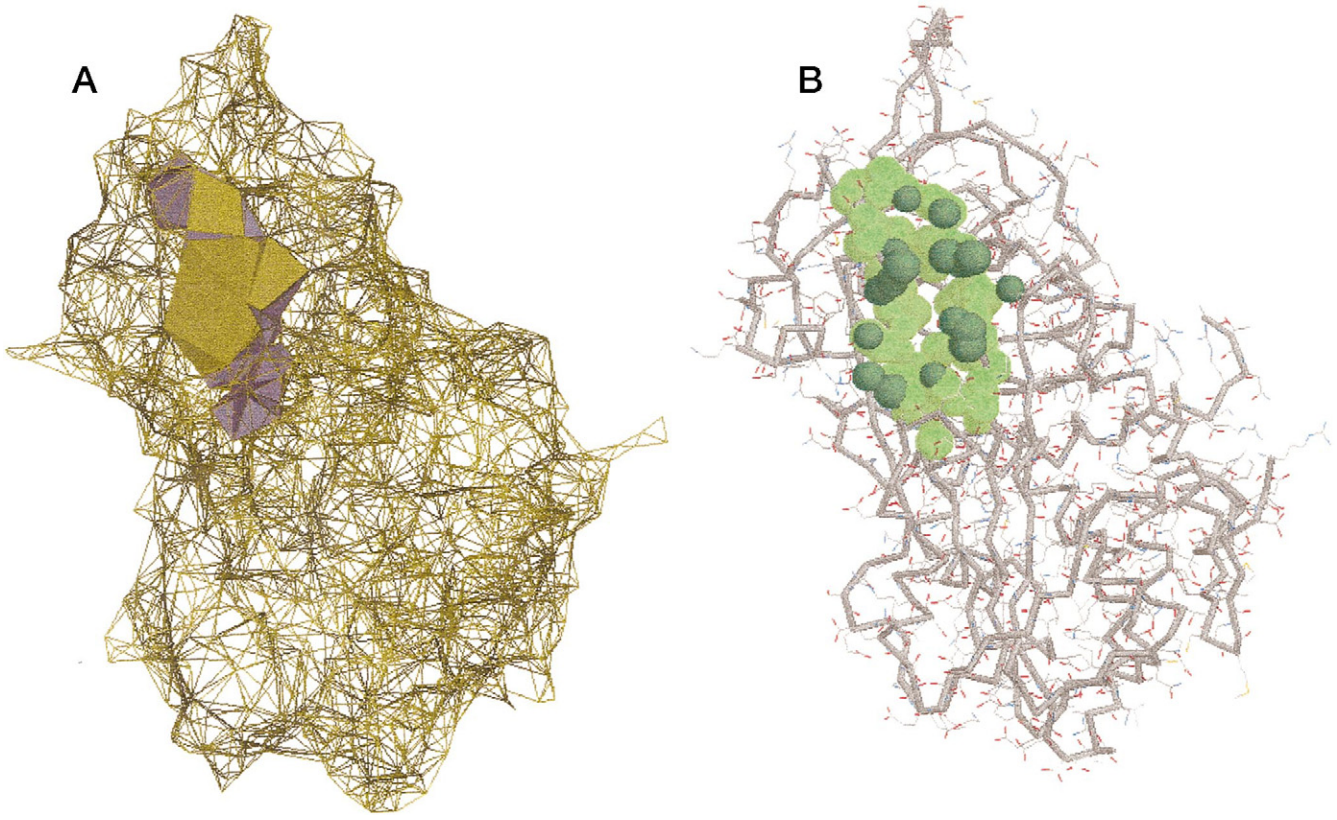

FIGURE 1 The largest pocket in the loop-exposed conformer of antithrombin. (*A*) The pocket is shown as a set of Delaunay tetrahedra, shaded in purple. The tetrahedra's triangular faces that correspond to the access pore or opening connecting the pocket concavity with solvent spaces are shaded in gold. (*B*) The same pocket is shown in space-filling rendition, with the atoms lining the pockets in green. The atoms bordering the access pore are in darker green.

heparin complex and factor Xa, and k is the first-order rate constant for conversion of reversible to stable complex. The dissociation constant for the interaction between AT and H is ~50 nM (Olson, 1988). The value of K is ~200 μM (Craig et al., 1989). At low concentrations of reactants (relative to K), the enzymatic activity of factor Xa decays exponentially according to the equation

$$k_{obs} = k[\mathrm{AT} - \mathrm{H}]/K \quad (1)$$

Measurement of water transfer during inhibition of factor Xa by antithrombin

Water transfer is measured with the OS technique. The technique's theoretical basis and general methodological approaches have been described in detail before (Parsegian et al., 1995). Briefly, reaction mixtures are equilibrated with cosolutes that are excluded from water-permeable spaces in the protein. The difference in water activity between excluded spaces and bulk solution generates an osmotic potential that favors water transfer from the excluded spaces to bulk solution. The component of the change in free energy of activation resulting from water transfer is determined from rate measurements at different concentrations of excluded cosolute. The volumes of water transferred are calculated from the ratio $\Delta(\Delta G^{\#})/\Delta\Pi$, between free energy change, $\Delta G^{\#}$, and osmotic pressure change, $\Delta\Pi$. Changes in free energy of activation are determined from the reaction rate coefficients according to classical thermodynamic relationships and the theory of rate processes (Glasstone et al., 1941).

To measure water transfer during factor Xa inhibition by antithrombin, reaction mixtures are equilibrated in the presence of inert cosolutes with molecular weights ranging from 98 to 500,000, including glycerol, mannitol, PEGs (with molecular weights ranging from 300 to 8000), PVP 40 (polyvinylpirrolidone, with a molecular weight of 40,000), DT 10, and DT 500 (dextran with molecular weights of 10,000 and 500,000). Osmotic pressures of DT500 and PVP 40 solutions are determined directly by membrane osmometry (Wescor 4420 colloid osmometer; Wescor, Logan, UT). The pressures generated by other cosolutes are extrapolated from published empirical relationships (Parsegian et al., 1995). Viscosities of PVP, PEG, and dextran solutions are measured with a calibrated cross-arm viscometer (Internal Research Glassware, Charlotte, NC). Dextran and PVP solutions were dialyzed extensively under back pressure as before (McGee and Teuschler, 1995). Purified human antithrombin, human factor Xa, and fractionated heparin were purchased from Enzyme Research Laboratories (South Bend, IN). Commercial grade heparin was from Sigma Chemical Co. (St. Louis, MO).

Salt titration experiments

The influence of OS on the electrostatic component of the reaction is examined by comparing effective charges between reactants in stressed ($\Delta\Pi$ = 1 atm, induced with PEG 3000) and control reaction mixtures. Mixtures contained fixed concentrations of antithrombin (98 nM), factor Xa (10 nM), and heparin (0.42 μg/ml ≈ 25 nM, estimated using a value of 17,000 to approximate the molecular weight of commercial grade heparin). Ionic strength was controlled with NaCl included in reaction mixtures at final concentrations ranging from 0.070 to 0.40 N. The effect of ionic strength, I, on reaction rates with and without osmotic stress is evaluated according to Bronsted's general formulation for reaction rates in salt

solutions (Glasstone et al., 1941; Scatchard, 1930):

$$k = k_0[\mathrm{AT-H}][\mathrm{Xa}]f_1f_2/f_3 \quad (2)$$

where k_0 is the rate coefficient under standard conditions, and f_1, f_2, and f_3 are the activity coefficients of [AT-H], [Xa], and [AT-H-Xa], respectively. Using the Debye-Huckel expression for the activity coefficient of ions in salt solutions and noting that the charge in the AT-H-Xa complex is the sum of charges in AT-H and Xa,

$$\ln f_1f_2/f_3 = 2.32\, z\, I^{1/2} \quad (3)$$

where z is the product of the charges in reactants. Together, Eqs. 2 and 3 predict a linear relationship between the natural logarithm of the reaction rate and the square root of the salt concentration. The product of the effective charges in reactants is calculated from the slope. Previous studies have demonstrated that decreases in the rate of protease inhibition with ionic strength are due primarily to screening of electrostatic interactions between antithrombin and heparin during formation of the initial ternary complex (Olson and Bjork, 1991; Olson et al., 1987).

Data analyses

Results of kinetic experiments were plotted and analyzed with computer programs Stat-view 512+ (Brain Power, Calabasas, CA) and kcat 3.1 (Biometallics, Princeton, NJ). Kinetic studies were repeated three to six times. Mean values and standard errors are indicated.

RESULTS

Hydration fingerprints of antithrombin conformers

The hydration fingerprints of human antithrombin conformers defined by the geometrical parameters of pockets in the x-ray structure are computed using α shape software. Fig. 2, *A* and *B*, shows pockets in the loop-exposed and loop-inserted conformer, respectively. Hydration fingerprints of each conformer are heterogeneous not only in volume and distribution of water-permeable spaces, but also in the area of pores connecting the pockets' concavities with the solvent spaces. The volumes of spaces with the capacity to hold at least two waters are listed in Table 1. The largest pocket that excludes PEG 300 has a capacity for 27 waters and is found in the loop-exposed, but not in the loop-inserted antithrombin conformer. The total volume of pockets and cavities that can accommodate water in the loop-exposed conformer is 3624 Å^3, enough for ~121 water molecules. The largest access pore in this conformer covers an area of 100 Å^2. In the loop-inserted conformer, the total volume of pockets and cavities is 2407 Å^3, and the largest access pore covers an area of 268 Å^2.

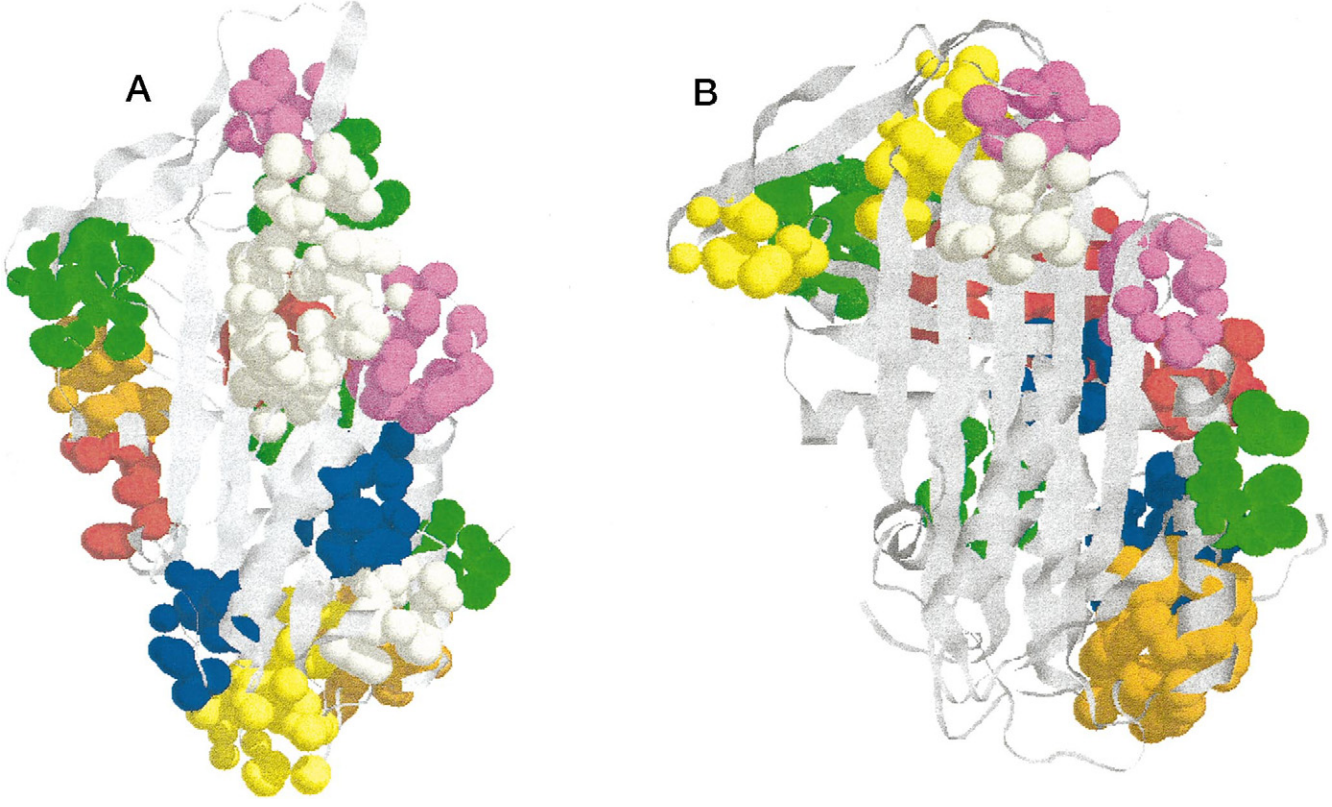

FIGURE 2 Hydration fingerprints of antithrombin conformers. The atoms forming pockets and cavities large enough to contain two water molecules are shown in space-filled balls superimposed on the backbone structure. Atoms forming each pocket are filled in the same color. Different pockets are distinguished as in a map, where neighbors have different colors. (*A*) Pockets in conformer with the loop exposed. (*B*) Pockets in conformer with loop inserted. Each conformer has distinct hydration fingerprints with very different sets of pockets. Differences include the number, size, and location of the pockets. (Note that similarly colored pockets in each conformer do not contain the same sets of atoms.) Quantitative characteristics of the pockets are in Table 1.

TABLE 1 Pockets and cavities in the two conformers of antithrombin

Loop-exposed conformer			Loop-inserted conformer		
Rank	Volume (Å^3)	Pore area (Å^2)	Rank	Volume (Å^3)	Pore area (Å^2)
1	818	100	1	683	268
2	445	86	2	349	19
3	432	83	3	220	55
4	288	37	4	210	69
5	201	52	5	196	64
6	199	51	6	125	59
7	188	53	7	98	23
8	181	24	8	97	15
9	160	0	9	84	0
10	136	66	10	76	0
11	125	71	11	73	29
12	123	35	12	72	0
13	89	0	13	63	64
14	85	56	14	60	21
15	77	0			
16	76	27			

The water-permeable spaces with a capacity for at least two water molecules in the two antithrombin conformers are ranked according to volume. The area of the access pore to each pocket is also indicated. Pockets with pore area 0 are closed cavities in the x-ray structure. Note that a probe such as PEG 300, with a radius length of 5.8 Å and cross-sectional area of 106 Å^2, is excluded from all pockets in both conformers, except the largest pocket in the loop-inserted conformer. The difference between conformers in pocket volumes that are inaccessible to this probe is 63 water molecules.

The number of water molecules is calculated from the volume and the water density in bulk solution. It is important to note that some of the hydration water may have a different density, particularly the water in immediate contact with the protein. It has been reported that water molecules near the protein surface occupy volumes up to 20% smaller than those in bulk solvent (Gerstein and Chothia, 1996).

Kinetics of factor Xa inhibition by antithrombin under osmotic stress

The rate of factor Xa inhibition by antithrombin is measured at different concentrations of protease, inhibitor, and heparin. Osmotic stress between 0 and 2.08 atm is induced with PEG 8000, with a molecular radius of ~2.6 nm (Atha and Ingham, 1981). Thus the molecular size of this cosolute is similar to that of antithrombin and larger than the access pore of all pockets. The free energy of activation decreases with pressure, indicating a net transfer of water from the proteins to bulk solution (Fig. 3 *A*). The slope of $\Delta G^{\#}/\Delta\Pi$ has at least two distinct linear segments of different length and with apparent discontinuities at $\Delta\Pi$ values of ~0.1 and ~0.5 atm. This heterogeneity suggests that the water transfer measured is from several spaces with diverse volumes and free energy contributions. Heterogeneity in free energy contribution of water transfer from different spaces is expected, because other processes take place concomitantly during the reaction. This interpretation is consistent with the volume heterogeneity of the water-permeable spaces in antithrombin functional domains as identified by α shape analysis. The total volume of water transfer, estimated from the first segment, is 1720 ± 536 cal/mol/atm, corresponding to 3800 molecules of water. (One atmosphere times the volume of 1 mole of water is equivalent to 0.453 cal.)

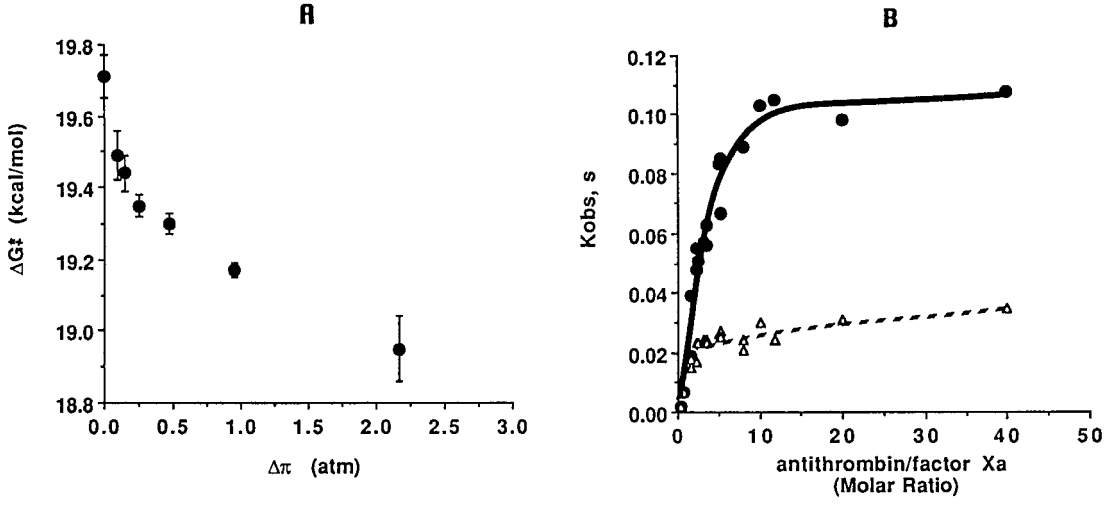

FIGURE 3 Factor Xa inhibition by antithrombin under osmotic stress. (*A*) Reaction mixtures contain fixed concentrations of factor Xa (10 nM), antithrombin (98 nM), heparin (0.4 μg/ml), and NaCl (0.07 N) and varying concentrations of PEG 8000 (0–12.5%), yielding the osmotic pressures indicated in the abscissa. The concentration of enzymatically active factor Xa is measured at different intervals with chromogenic substrate. Pseudo-first-order rate coefficients, k_{obs}, are obtained by fitting exponential decay curves to data points. Changes in free energy of activation, $\Delta G^{\#}$, are calculated from ln k_{obs} at each pressure level according to transition-state theory. Data points in the figure are the mean values and standard error from three independent determinations. (*B*) Rates were measured in mixtures with (●) and without (△) PEG (8.3%, $\Delta\Pi \approx 1$ atm), and with antithrombin (11–440 nM) and factor Xa (10–58 nM) at the molar ratios indicated in the abscissa. Other components and conditions are as indicated in *A*. Rectangular hyperbolas fitted to data points gave $K_{1/2}$ values (i.e., AT/Xa ratio at half-maximum rate) of 4.15 ± 0.80 and 1.82 ± 0.35 with and without PEG, respectively.

In titrations with either factor Xa or antithrombin, the increase in k_{obs} with osmotic stress is at maximum when antithrombin is in molar excess over factor Xa (Fig. 3 *B*). Second-order rate coefficients calculated from the initial slope of the titration curves are 2.0 ± 0.29 and $1.0 \pm 0.25 \times 10^6\ M^{-1}\ s^{-1}$ with and without osmotic stress. Stoichiometry of AT-H-Xa complex, determined from residual factor Xa activity in titrations with antithrombin at fixed heparin concentrations (Olson et al., 1993), is 1.29 ± 0.11 and 1.21 ± 0.04 with and without OS. This result indicates that OS does not induce aggregation or precipitation of the reactants. In titrations with heparin, the k_{obs} increases with the heparin concentration, but the effect of osmotic stress (that is, the fold increase in k_{obs}) does not change significantly with heparin within the range of concentrations tested. Average fold increases at $\Delta\Pi \approx 1$ atm are 2.6 ± 0.2 and 4.4 ± 0.5 for heparin concentrations ranging from 6 to 96 nM with commercial grade heparin and from 0.5 to 8 μM with fractionated heparin. Osmotic stress does not change the rate of chromogenic substrate hydrolysis by factor Xa.

Reaction rates under OS induced with PEG of graded sizes

The volume of water transfer measured with PEG 8000 exceeds the total volume in water-permeable pockets and cavities measured in the crystal structure by computational geometry. This suggests that such a large probe detects water transfer from larger interfacial spaces formed between factor Xa and antithrombin during stabilization of the reaction complex. To test this possibility, OS experiments were repeated with PEG of different sizes. The purpose is to identify probes excluded from protein pockets but with access to larger interprotein solvent spaces (Table 2). Water transfer measured with PEG 300 falls within the required range, as determined from the difference between the volume in the pockets of the two antithrombin conformers (Table 1).

The volume of water transfer measured with larger cosolutes increases progressively with the size of cosolute up to probes with radius ~20 Å. Larger probes result in similar volume transfer. The volumes measured with DT 10, DT 500, PEG 8000, and PVP 40 over the pressure range 0–0.1 atm (the range that is experimentally accessible with the four cosolutes) are not significantly different (Table 2). Thus, for cosolutes with large molecular radii relative to the size of the reacting proteins, the osmotic effect is independent of the cosolute's size, suggesting complete exclusion from all water-permeable spaces. At the other extreme, probes with a radius below ~3 Å do not change reaction rates significantly, consistent with complete penetration of both inter- and intraprotein spaces. Results in Table 2 also show that the effect on reaction rates is independent of the solutions' viscosity and of the cosolutes' chemical composition.

TABLE 2 Water transfer measured with cosolutes of different sizes and chemical compositions

Cosolute	Molecular weight	Slope $\Delta G^{\#}/\Delta\Pi$ (cal/mol/atm)	No. of water molecules*
Glycerol	92	0	0
Mannitol	182	0	0
PEG	300	33 ± 3	74
	400	46 ± 9	102
	600	57 ± 5	130
	1000	109 ± 13	251
	1500	201 ± 30	462
	3400	540 ± 50	1241
	8000	1720 ± 536	3801
DT	10000	1850 ± 712	4088
	500000	2411 ± 1010	5328
PVP	40000	2370 ± 125	5255

* The rate of factor Xa inhibition by antithrombin was measured under osmotic stress induced with the cosolutes indicated. Molecular weights listed are average values provided by the suppliers. Changes in free energy of activation were determined from reaction rate coefficients at different osmotic stress levels, as indicated in the legend to Fig. 3. The number of water molecules transferred was calculated from the initial slope (1 atm times the volume of 1 mole of water is equivalent to 0.435 cal).

Electrostatic interaction under osmotic stress

To examine the electrostatic component of reactions under OS, reaction rates are measured at different NaCl concentrations, ranging from 0.050 to 0.25 N, with and without 6.7% PEG 3400 ($\Delta\Pi \approx 1$ atm). Osmotic stress has only a small effect on effective electrostatic parameters. Plots of ln k_{obs} versus $I^{1/2}$ are linear with slopes of -1.9 ± 0.21 and -3.1 ± 0.15, with and without OS, respectively. The product of effective charges calculated from the slope is 0.82 ± 0.09 and 1.35 ± 0.15 with and without OS.

Location and volume of water-permeable spaces excluded by PEG 300

The volumes of water-permeable spaces excluding PEG 300 are calculated from the differences between the volumes accessible to probes of 1.4-Å and 5.8-Å radii, representing water and cosolute, respectively. The volumes are derived analytically from the molecular surface (Connolly surface) swept spheres with radii of either size. Consistent with the information provided by the hydration fingerprints, this cosolute size is excluded from many small pockets and cavities in the loop-exposed conformer. The residues associated with these spaces are indicated in Fig. 4. The spaces that exclude this size cosolute are located in functional and mobile domains of antithrombin, including the reactive loop and the large pocket in the loop insertion region of the exposed conformer.

Difference in excluded volumes between antithrombin conformers

Osmotic stress measurements using PEG 300 indicate a transfer of 73.6 molecules of water from the proteins to the

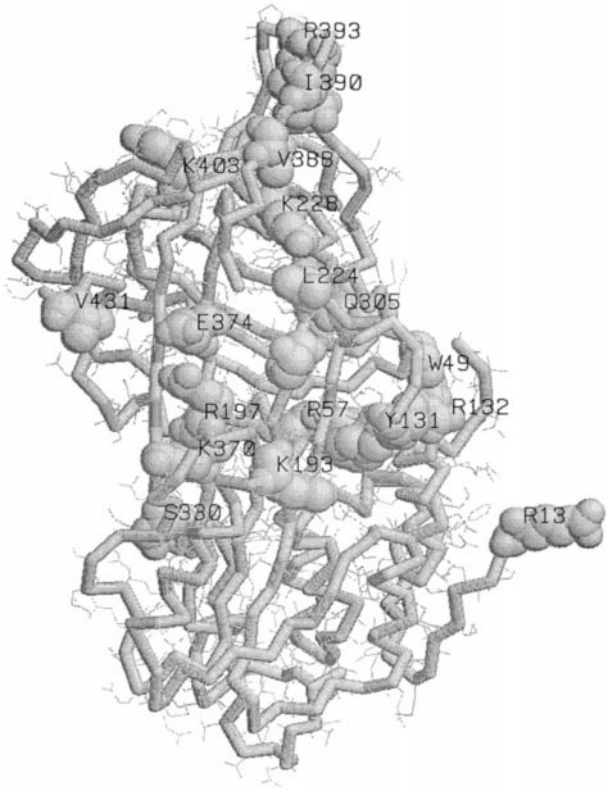

FIGURE 4 Location of residues associated with water spaces that exclude a probe with 5.8-Å radius. To facilitate visualization, only the residues with the 20 highest water volumes are indicated. These residues are represented as space-filling balls labeled with the one-letter code and superimposed on the backbone.

TABLE 3 Water-permeable spaces of antithrombin excluded by a probe with 5.8 Å^2 radius

Residue	Volume* difference (Å^3)
Glu^{104}	66.647
Pro^{288}	67.446
Leu^{224}	67.647
Glu^{357}	73.958
Ile^{22}	74.706
Asn^{376}	76.668
Asp^{72}	77.944
Phe^{372}	81.466
Glu^{374}	81.601
Tyr^{131}	81.771
Ser^{330}	85.391
Glu^{255}	86.624
Glu^{232}	87.904
Ala^{383}	91.385
Arg^{46}	92.104
Arg^{132}	93.993
Arg^{395}	96.573
Trp^{49}	121.233
Val^{388}	154.507
Il^{390}	184.324

* Differences are for residues losing at least two water molecules, i.e., >60 Å^3.

Residues have more water in loop-exposed than in loop-inserted conformer.

bulk solution during the reaction (Table 2). To determine if the water transfer measured with OS is associated with loop insertion, we analyze the differences between the water-permeable spaces in the two conformers of antithrombin. Volumes that exclude probes with either 3 Å or 5.8 Å radii (lower and upper estimates for the radii of PEG 300) are measured in both antithrombin conformers. There is an excess of 56 and 76 water molecules (detected with the 3-Å and 5.8-Å probe, respectively) in the loop-exposed conformer. Using only residues that are resolved in both structures, the volumes correspond to 49 and 61 waters, respectively. The residues associated with the water differences are listed in Table 3, and their relative location in the structure is illustrated in Fig. 5. These values are fully consistent with results obtained by comparing the volume of pockets in the hydration fingerprints of the two conformers. Pockets with access pores smaller than the cross-sectional area of the probe contain 63 more waters in the exposed, as compared to the inserted, conformer (Table 1).

DISCUSSION

This study demonstrates that inhibition of coagulation factor Xa by antithrombin is associated with a net transfer of water from the proteins to bulk solution. It also illustrates the combined use of osmotic stress and analytical geometry as a new and effective tool for structure/function studies.

Analysis of the hydration fingerprints of the x-ray structures of antithrombin indicates that the volume of water-permeable spaces is larger in the loop-extended antithrombin conformer. The magnitude of the volume difference measured in the structures correlates closely with the net volume of water transfer measured by OS. The size limit of the probe excluded from the water-permeable pockets in antithrombin structure is determined from the area of the access pores. This area is calculated analytically from the atomic coordinates. Approximately half of the water measured by osmotic stress can be accounted for by the volume of the largest pocket in the loop domain of antithrombin.

The effect of osmotic stress is associated primarily with the stabilization of the initial protease-inhibitor complex. This is deduced from the OS effect observed at different reactant concentrations. At low antithrombin/factor Xa ratios, the value of k_{obs} is dominated by the value of [AT.H] (see Experimental Procedure). With [AT] in excess of heparin and factor Xa concentrations, but still small relative to K, k_{obs} becomes independent of [AT]. Therefore, if OS were to increase k_{obs} by increasing [AT-H-Xa], the effect would be larger (or the same) at low rather than at high concentrations of antithrombin. Instead, the increases in k_{obs} with OS are observed when antithrombin is in excess of factor Xa and heparin.

Additional support for the role of water transfer during the stabilizing transition is derived from results of salt titration experiments. Increasing the ionic strength of the

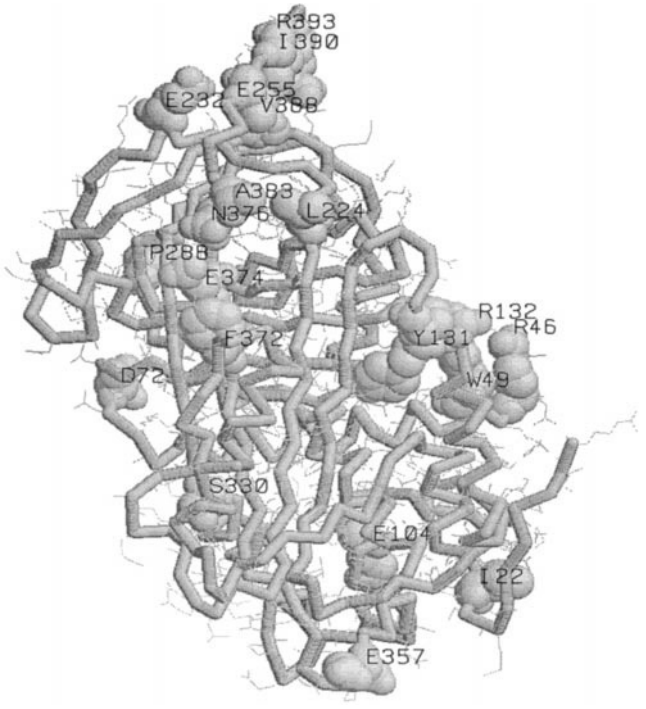

FIGURE 5 Residues that lose at least two water molecules on passing from exposed to inserted conformation. Residues are depicted on the loop-exposed conformer. Note how some of the residues that lose water are not associated with pockets, for example, R393 and I390 in the loop region. (The total volume of water-permeable spaces in the loop-exposed conformer is 15,532 Å^3 and is sufficient to accommodate ~517 water molecules. The corresponding volumes in the inserted conformer are 13,216 Å^3, sufficient for 440 water molecules. These total volumes are different from volumes accounted for by the pockets in that they also include the hydration layer of shallow depressions and flat surfaces.)

reaction environment from 0.07 to 0.25 decreases reaction rates severalfold, but modifies $\Delta G^{\#}/\Delta\Pi$ coefficients only slightly. Therefore, the increase in reaction rates with osmotic stress is not due to effects on electrostatic interactions. Studies by others have demonstrated that electrostatic forces are a major component of the total free energy for the antithrombin and heparin interaction (Olson and Bjork, 1991). In our experiments, the slope of k_{obs} versus $I^{1/2}$ increases by 37% when OS is applied. This small increase in slope with OS is consistent with a salt-sensitive step that is stabilized by water. Some change in the equilibrium position between antithrombin and heparin is also suggested by the small but significant increase in concentration, yielding half-maximum rates with OS in titrations with antithrombin (Fig. 3 *B*). Under the conditions of the experiments, this observation reflects an increase in the dissociation constant of AT-H interaction (Olson and Bjork, 1994) and suggests that water is also transferred during heparin's activation of antithrombin. However, the transfer at this reaction step is from bulk solution to reactants and is small in magnitude. Structural data also show that some antothrombin residues are more hydrated in the fully inserted conformer than in the partially inserted conformer. Interestingly, several of these residues are either hydrophobic or neutral (Table 4) and are located near the shutter regions in sheets 3B and 3C (Schreuder et al., 1994; Carrel et al., 1994).

The values of excluded volumes in antithrombin conformers determined by α shape analysis are qualitatively and quantitatively consistent with the limiting values of water transfer determined by osmotic stress. This finding strongly suggests that the excess water detected functionally by osmotic stress can be explained by changes in antithrombin water-permeable spaces during loop insertion. Most of the large pockets that exclude the 5.8-Å probe are located at the loop and loop-insertion regions. The pockets are smaller in the fully inserted, as compared to the partially inserted or loop-exposed, conformer. Thus, from objective geometrical criteria alone, it again follows that loop insertion in solution is associated with water transfer from antithrombin to bulk.

Considering the approximations involved in assigning sizes to water and cosolute for α shape analysis as well as the unavoidable errors in the measurement of osmotic pressure, the quantitative correspondence between volume values must be interpreted with caution. Both values represent net changes in excluded volume. It is possible that a fraction of the volume of water transfer measured during reactions is from factor Xa. However, the rate of small substrate hydrolysis by factor Xa is not affected by OS. This observation suggests that occupation of the protease active site during functional interactions does not result in a large change to its water-permeable volumes. At present, there is no indication that conformational changes in factor Xa are comparable in scale to those in antithrombin. Questions about the relative contribution of the protease to the volumes of water transfer measured by osmotic stress may be resolved when additional structures of factor Xa conformers and antithrombin-factor Xa complexes become available.

Our results also suggest that water transfer to bulk measured with large cosolutes is mainly from intermolecular spaces enclosed by the approaching proteins. The existence of large interprotein spaces during the reaction is inferred from the differential effects observed with cosolutes of graded size. Both large and small cosolutes are excluded

TABLE 4 Residues with more water in the loop-inserted than in loop-exposed conformation

Residue	Volume difference (Å^3)
Leu^{285}	127.890
Asn^{73}	108.086
Phe^{239}	107.297
Asn^{45}	106.690
Leu^{152}	87.711
Asn^{178}	86.594
Lys^{294}	80.049
Lys^{432}	75.065
Leu^{173}	74.287
Lys^{53}	73.391
Asn^{127}	68.082
Ser^{230}	66.331

from flat surfaces and shallow pockets (Hermans, 1982). However, transfer of large volumes is detected only with large cosolutes. Most of the water transfer detected by small cosolutes can be accounted for by changes in the pockets. When total volumes of water-permeable spaces are measured by rolling a water probe over the whole molecule, the values obtained are larger than the sum of the volumes of the pockets. This is expected, because the hydration layers of shallow and flat surfaces are now included. However, the volume difference between conformers is maintained. Taken together, these data agree that large interprotein spaces are formed in the ternary complex and are fully accessible to PEG 300, but not to larger cosolutes.

It has been proposed that the structure of antithrombin with a partially inserted loop best reflects the conformation of antithrombin in solution (van Boekel et al., 1994). In this model, heparin binding is associated with expulsion of the inserted residues, resulting in a fully exposed and flexible reactive loop (Huntington et al., 1996). This flexible conformation increases the affinity of antithrombin for factor Xa and modifies the spectroscopic and immunogenic characteristics of antithrombin. Antithrombin then undergoes a large conformational change that includes the reinsertion of the reactive loop into the β-sheet. This leads to irreversible inhibition of factor Xa and the release of heparin. The results presented here confirm and expand these proposed mechanisms. There is a net transfer of water, measured both in the structures by computational geometry and during the reaction by osmotic stress. The transfer of water from antithrombin to the bulk solution is associated with loop reinsertion during the stabilizing step of the inhibitory reaction.

The structure and function of antithrombin have been linked, using water as a common probe both to define biologically relevant structural resolutions and to characterize the role of solvent during functional interactions.

This research was supported by a grant from the National Science Foundation (MCB-9601411).

REFERENCES

Arakawa, T., and S. N. Timasheff. 1985. Mechanisms of polyetylene glycol interaction with proteins. *Biochemistry.* 24:6756–6762.

Atha, D. H., and K. C. Ingham. 1981. Mechanism of precipitation of proteins by polyethylene glycols. *J. Biol. Chem.* 256:12108–12117.

Aurenhammer, F. 1991. Voronoi diagrams—a survey of fundamental geometric data structure. *ACM Comput. Surv.* 23:345–405.

Bryant, R. G. 1996. The dynamics of water-protein interactions. *Annu. Rev. Biophys. Biomol. Struct.* 25:29–53.

Carrell, R. W., and D. R. Boswell. 1986. Serpins: the superfamily of plasma serine proteinase inhibitors. *In* Proteinase Inhibitors. A. J. Barret and G. Salveson, editors. Elsevier Science Publishers, Amsterdam. 403–420.

Carrel, R. W., and P. Stein. 1996. The biostructural pathology of serpins: critical function of sheet opening mechanism. *Biol. Chem. Hoppe Seyler.* 377:1–17.

Carrell, R. W., P. E. Stein, G. Fermi, and M. R. Wandell. 1994. Biological implications of a 3 Å structure of dimeric antithrombin. *Structure.* 2:257–270.

Connolly, T. 1983. Analytical molecular surface calculation. *J. Appl. Cryst.* 16:548–558.

Craig, P. A., S. T. Olson, amd J. D. Shore. 1989. Transient kinetics of heparin-catalyzed protease inactivation by antithrombin III: characterization of assembly, product formation, and heparin dissociation steps in the factor Xa reaction. *J. Biol. Chem.* 264:5452–5461.

Delaunay, B. 1934. Sur la sphere vide. Izvestia Akademii Nauk SSSR, *Otdelenie Matematicheskii Estestvennyka Nauk.* 7:793–800.

Edelsbrunner, H., and E. Mucke. 1990. Simulation of simplicity: a technique to cope with degenerate cases in geometric algorithms. *ACM Trans. Graph.* 9:66–104.

Edelsbrunner, H., and E. Mucke. 1994. Three-dimensional alpha shapes. *ACM Trans. Graph.* 13:43–72.

Edelsbrunner, H., M. Facello, P. Fu, and J. Liang. 1995. Measuring proteins and voids in proteins. *In* Proceedings of the 28th Annual International Conference on System Sciences, Vol. 5. IEEE Computer Society Press, Los Alamitos, CA. 256–264.

Edelsbrunner, H., M. Facello, and J. Liang. 1996. On the definition and the construction of pockets in macromolecules. *In* Proceedings of the First Pacific Symposium on Biocomputing. World Scientific, Singapore. 272–281.

Edelsbrunner, H., and N. Shah. 1995. Incremental topological flipping works for regular triangulations. *In* Proceedings of the 8th Annual Symposium on Computer Geometry. ACM Press, New York. 43–52.

Facello, M. 1995. Implementation of a randomized algorithm for Delaunay and regular triangulation in three dimensions. *Computer Aided Geometric Design.* 12:349–370.

Glasstone, S., K. Laidler, and H. Eyring. 1941. The Theory of Rate Processes. McGraw-Hill, New York and London. 1–27.

Gerstein, M., and C. Chothia. 1996. Packing at the protein-water interface. *Proc. Natl. Acad. Sci. USA.* 93:10167–10172.

Gerstein, M., J. Tsai, and M. Levitt. 1995. The volume of atoms on the protein surface: calculated from simulation, using Voronoi polyhedra. *J. Mol. Biol.* 249:955–966.

Hermans, J. 1982. Excluded volume theory of polymer-protein interaction based on polymer chain statistics. *J. Chem. Phys.* 77:2193–2203.

Huntington, J. A., S. T. Olson, F. Bingqi, and P. G. Gettins. 1996. Mechanism of heparin activation of antithrombin. Evidence for reactive center loop preinsertion with expulsion upon heparin binding. *Biochemistry.* 35:8495–8503.

Israelachvili, J., and H. Wennerstrom. 1996. Role of hydration structure in biological and colloidal interactions. *Nature.* 379:219–342.

Kim, S., J. Liang, and B. A. Barry. 1997. Chemical complementation identifies a proton acceptor for redox-active tyrosine D in photosystem II. *Proc. Natl. Acad. Sci. USA.* 94:14406–14411.

Kuznetsova, N., D. C. Rau, V. A. Parsegian, and S. Leikin. 1997. Solvent hydrogen-bond network in protein self-assembly: solvation of collagen triple helices in non-aqueous solvents. *Biophys. J.* 72:353–362.

Liang, J., H. S. Edelsbrunner, P. Fu, P. Sudhakar, and S. Subramanian. 1998a. Analytical shape computation of macromolecules. I. Molecular area and volume through alpha shape. *Proteins.* (in press).

Liang, J., H. S. Edelsbrunner, and C. Woodward. 1998b. Anatomy of protein pockets and cavities: measurement of binding site geometry and implications for binding desing. *Protein Sci.* (in press).

Liang, J., and S. Subramaniam. 1997. Computing molecular electrostatics through boundary element method. *Biophys. J.* 73:1830–1841.

McGee, M. P., and L. C. Li. 1991. Functional difference between intrinsic and extrinsic coagulation pathways. *J. Biol. Chem.* 266:8079–8085.

McGee, M. P., and H. Teuschler. 1995. Protein hydration during generation of coagulation factor Xa in aqueous phase and phospholipid membranes. *J. Biol. Chem.* 270:15170–15174.

Olds, R. J., D. A. Lane, B. Miller, V. Chowdhury, and S. L. Thein. 1994. Antithrombin, the principal inhibitor of thrombin. *Semin. Thromb. Hemost.* 20:353–372.

Olson, S. T. 1998. Transient kinetics of heparin-catalyzed protease inactivation by antithrombin III: linakage of protease-inhibitor-heparin interactions in the reaction with thrombin. *J. Biol. Chem.* 263:1698–1708.

Olson, S. T., and I. Bjork. 1991. Predominant contribution of surface approximation to the mechanism of heparin acceleration of antithrombin-thrombin reaction. *J. Biol. Chem.* 266:6353–6364.

Olson, S. T., and I. Bjork. 1994. Regulation of thrombin activity by antithrombin and heparin. *Semin. Thromb. Hemost.* 20:373–409.

Olson, S. T., I. Bjork, P. Craig, G. D. Shore, and J. Choay. 1987. Role of high-affinity pentasaccharide in heparin acceleration of antithrombin III inhibition of thrombin and factor Xa. *Thromb. Haemost.* 58:8a.

Olson, S. T., I. Bjork, and J. D. Shore. 1993. Kinetic characterization of heparin-catalyzed and uncatalyzed inhibition of blood coagulation proteinases and antithrombin. *Methods Enzymol.* 222:525–559.

Parsegian, V. A., R. P. Rand, and D. C. Rau. 1995. Macromolecules and water: probing with osmotic stress. *Methods Enzymol.* 259:43–94.

Peters, K. P., J. Fauk, and C. Frommel. 1996. The automatic search for ligand binding sites in proteins of known three dimensional structure using only geometrical criteria. *J. Mol. Biol.* 256:201–213.

Rand, R. P. 1992. Raising water to new heights. *Science.* 256:618.

Richards, F. M. 1997. Areas, volume packing and protein structure. *Annu. Rev. Biophys. Bioeng.* 6:151–176.

Scatchard, G. 1930. The rate of reaction in a changing environment. *J. Am. Chem. Soc.* 52:52–61.

Schreuder, H. A., B. de Boer, R. Dijkema, J. Mulders, P. D. J. Theunissen, H. J. M. Grootenhuis, and W. G. J. Hol. 1994. The intact and cleaved human antithrombin complex as a model for serpin-proteinase interactions. *Struct. Biol.* 1:48–54.

Squire, P. G., and M. E. Himmel. 1979. Hydrodynamics and protein hydration. *Arch. Biochem. Biophys.* 196:165–177.

van Boeckel, C. A., P. D. Grootenhuis, and A. Visser. 1994. A mechanism for heparin-induced potentiation of antithrombin III. *Nat. Struct. Biol.* 1:423–425.